

Original Paper

## SR Embrittlement and Temper Embrittlement Observed in HAZ of 2¼Cr-1Mo Steel

Koreaki TAMAKI, Jippei SUZUKI, Hiroshi KAWAKAMI  
Kazuhiro TANAKA  
(Department of Mechanical Engineering)

(Received September 18, 1995)

### Abstract

The temper embrittlement of HAZ of 2 1/4Cr-1Mo steel was studied in the tempering temperature – time range of 775 to 975K and 0.2 to 10000 hours. The changes of transition temperature and fracture mode informed that there were five types of temper embrittlement. The fifth type of temper embrittlement arose in the temperature range higher than 950K and the other four types did in the temperature range lower than 900K. The first and second types arose in the earlier tempering stages, such as the tempering time shorter than 100hr at 825K. The third and fourth types were observed in the later tempering stages, such as the tempering times longer than 100hr and 1000hr, respectively at 825K. The third type exhibited the fracture mode of intergranular, but other four types did that of transgranular. The third type and fifth type will be identical with the reversible temper embrittlement and SR embrittlement. Little attention has been paid on the embrittlement of the types of first, second and fourth, and hence little is known on the characteristics of those types of embrittlement.

### Key words

Cr-Mo steels, heat affected zone, temper embrittlement, SR embrittlement, new types of embrittlement, transition temperature, fracture mode.

### 1. Introduction

2 1/4 Cr-1Mo steel is an important heat-resisting material and applied most widely to the boilers and the pressure vessels. These apparatuses are constructed by means of several arc welding processes. The heat affected zone (HAZ) of the weldment, however, was

occasionally embrittled after a long-time service of the apparatus. This phenomenon was known as the temper embrittlement which arose in the temperature range around 820K [1,2].

Another type of temper embrittlement arises when the weldments are heat-treated at about 970K for relieving the residual stress; the term "SR embrittlement" was given to this type of temper embrittlement [3].

Most of the preceding researches used the experimental procedure that the quenched specimen was tempered at first at 875K for obtaining "the de-embrittled" specimen (the specimen of which the brittleness produced by the preceding heat treatment was removed), and then the specimen was tempered again at a given temperature, or slow-cooled from 875K. In this procedure, however, the embrittlement which may occur during the heating process up to 875K is completely neglected.

In this research, the authors adopted the experimental procedure that the HAZ specimen of as-quenched state was tempered at each given temperature and time. The occurrence of temper embrittlement was detected by "the rise of transition temperature" which was given by the impact test. SEM observations were conducted on the specimen broken by the impact test.

As the results of this research, five types of temper embrittlement were found. The temperature-time ranges where they arose were shown graphically in a diagram.

Some discussions were made on the natures of those types of temper embrittlement referring to the data of previous researches.

## 2. Experimental system

### 2.1 Simulated-HAZ specimen

2 1/4Cr-1Mo steel plate (JIS SCM4V) of 13mm in thickness was used; its chemical compositions are shown in Table 1. This steel was supplied in the quench-tempered condition.

The microstructure of HAZ given by bead-welding with the following welding conditions was reproduced in a steel bar by using a weld-thermal-cycle simulator.

**Table 1 Chemical composition of 2 1/4Cr-Mo steel plate (wt%)**

C	Si	Mn	P	S	Ni	Cr	Mo	Cu	As
0.14	0.16	0.56	0.006	0.002	0.03	2.17	0.90	0.01	0.004

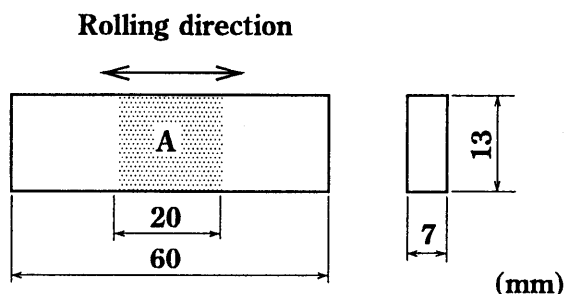


**Fig.1 Steel bar for preparing the HAZ specimen**

**A:Area where an uniform microstructure is produced**

arc voltage 24V, welding current 180A, welding speed 15cm/min, heat input 17.3kJ/cm, without preheating.

The HAZ contains 75% bainite and 25% martensite with the hardness of 360 Hv. The simulated-HAZ was obtained by the heating rate of 92K/s, the cooling rate 21K/s and the ultimate temperature 1623K [4]. The size of steel bar for preparing simulated-HAZ specimen (briefly written as HAZ specimen) is shown in Fig.1; the center portion of 20mm in length reserves an uniform microstructure.

## 2.2 Heat treatment of specimen

The temper embrittlement appears in some alloy steels when they are quenched and tempered in a certain temperature range; the embrittlement is intensified when the tempered steels are cooled slowly. Several heat treatments have been used for revealing the temper

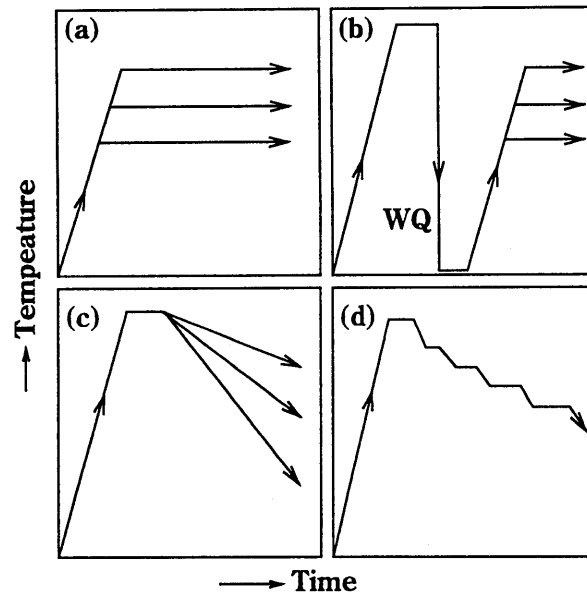


**Fig.2 Experimental programs used for revealing temper embrittlement**

- (a) Direct-isothermal tempering,
- (b) Isothermal tempering after the de-embrittling treatment,
- (c) Slow cooling from the de-embrittled state,
- (d) Step-cooling from the de-embrittled state

embrittlement in laboratories. Fig.2 (a) shows the direct-isothermal tempering; this heat treatment is most similar to that used for real engineering process. Another method of isothermal tempering is shown in Fig.2 (b). At first, the specimen is tempered at about 875K for obtaining the de-embrittled state. The water-quenched specimen is tempered again at each given temperature. Fig.2 (c) shows the method that the specimen is slow-cooled from the de-embrittled state. Fig.2 (d) explains another method of slow-cooling (the step-cool-

ing), in which the specimen is cooled stepwise [5].

In the method of direct-isothermal tempering (Fig.2 (a)), some complicity arises that the microstructure is varied by the progressive tempering process and it may affect the experimental result of embrittlement. However, this method alone has an important advantage that it can detect some types of embrittlement which arise in the real tempering process from the as-quenched condition to the full-tempered one. The direct-isothermal tempering was adopted in this research.

One group of HAZ specimens (twenty to fifteen specimens) were enclosed in a steel box (50x95x100mm), and they were tempered at 775 to 975K (nine levels of temperature) for 0.2 to 10000 hours (fourteen intervals of time) in an electric-resistance furnace. After the tempering, the steel box was removed from the furnace and cooled in air. The cooling rate of the specimen itself was about 60K/min.

### 2.3 Charpy impact test

A half-size Charpy impact-test specimen of Fig.3 was made from the tempered HAZ specimen. The temperature range of impact test was 95K to 320K. The temperature of specimen was controlled by the following methods. Above room temperature: the specimen was warmed in a water bath. Above 185K: the specimen was cooled in an ethyl alcohol bath cooled by liquid nitrogen. Below 185K: (1)Alumel-chromel thermocouple was attached to the specimen, and the latter was cooled as low as 77K by liquid nitrogen. (2)The cooled specimen was placed on the supporting anvil of impact-test machine and its temperature is left rising. (3)The specimen was broken when the given temperature was attained.

The capacity of the impact-test machine was 98J (10kgf-m).

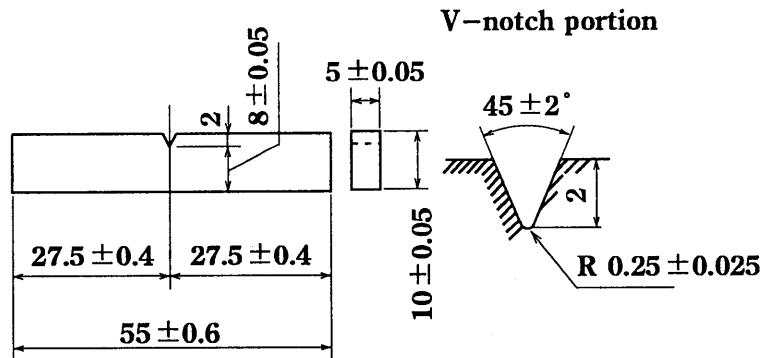


Fig.3 Specimen for Charpy impact test

## 3. Result of impact test

### 3.1 Transition temperatures of base metal and HAZ specimens

Fig.4 (a) and (b) show the transition curves of absorbed energy of the base metal in as-received condition and the HAZ specimen. The absorbed energy of base metal is transferred steeply from the upper-shelf value to the lower-shelf one in a very narrow temperature range (Fig.4 (a)). The transition curve of HAZ specimen differs from that of base metal such that: (1) the upper-shelf energy is smaller, (2) the transition occurs in two steps at about

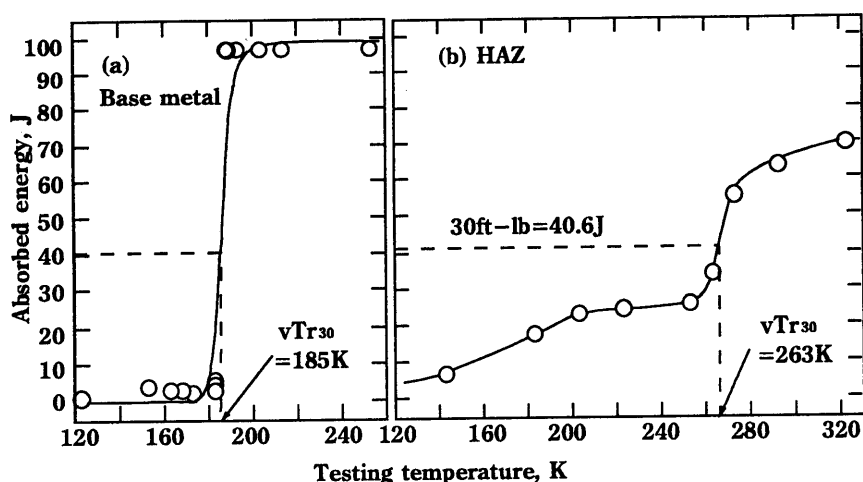


Fig.4 Energy-transition curves of base metal (a) and HAZ(b)

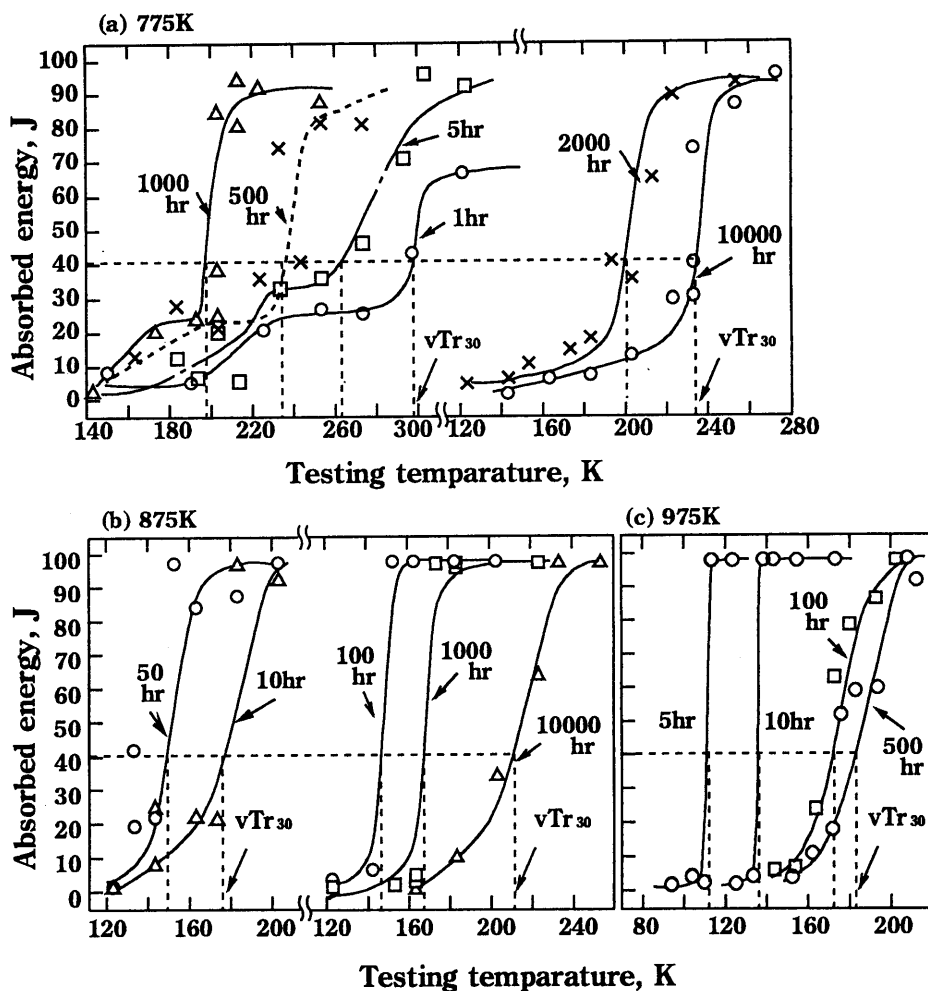


Fig.5 Energy-transition curves of three groups of specimens tempered at 775K(a), 875K(b) and 975K(c)

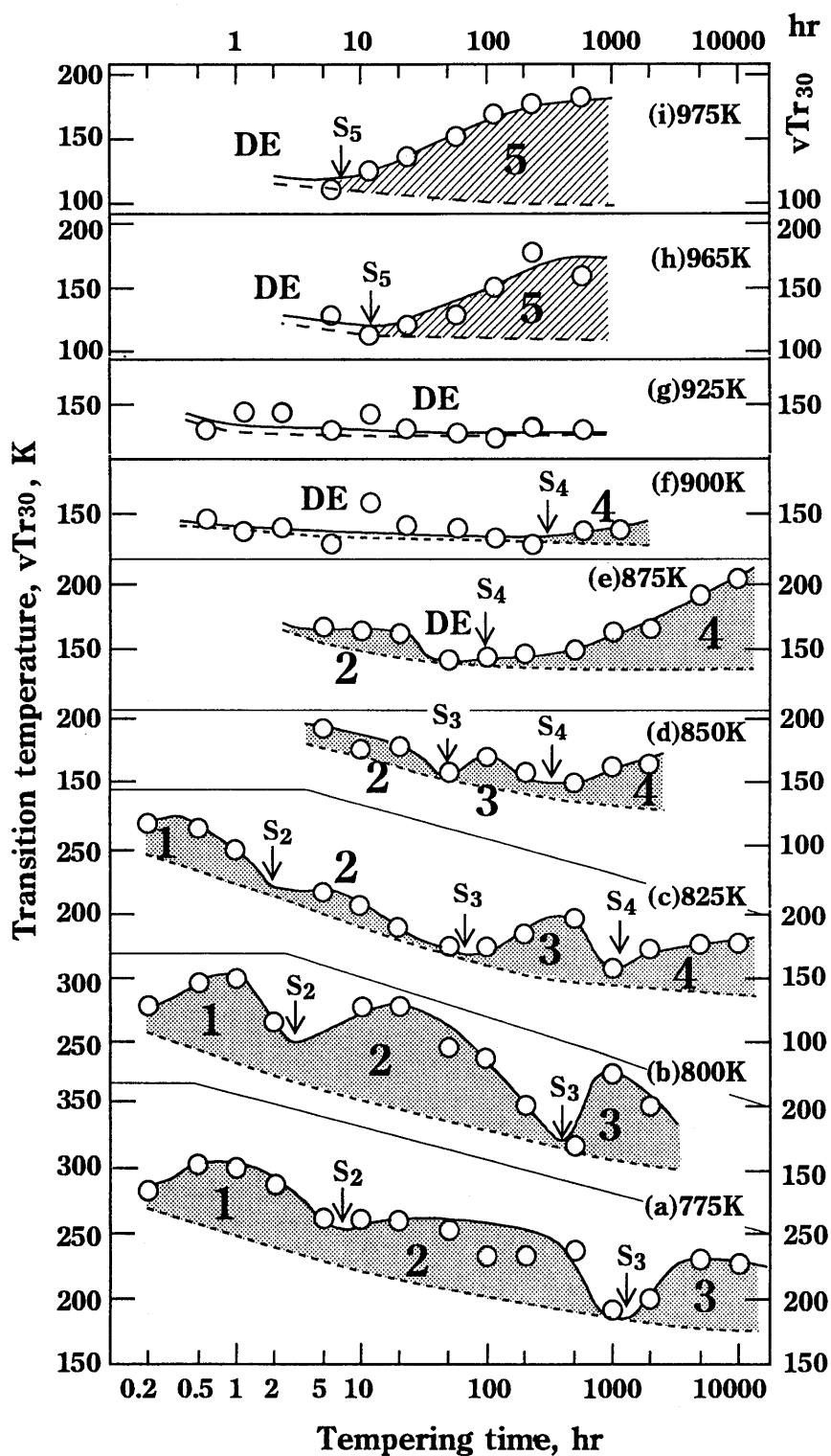


Fig.6 Temper embrittlement observed as the rise of  $vTr_{30}$  in each  $vTr_{30}$ -tempering time curves

260K and 180K.

The authors adopted the temperature which gave 30ft-lb(40.6J) of absorbed energy as the energy-transition temperature in this research. This transition temperature,  $vTr_{30}$ , indicates well the first step of transition as shown in Fig.4 (b).

The  $vTr_{30}$  values of base metal and HAZ are 185K and 263K, respectively.

### 3.2 Change of transition temperature with the progress of tempering

#### (a) Examples of transition curves

Three groups of transition curves are shown in Fig.5. Transition curves of specimens tempered at 775K for 1 to 1000 hours show two steps of transition, this manner of transition is very similar to the case of the HAZ specimen (Fig.5(a)). The  $vTr_{30}$  of this group is lowered with an increasing tempering time up to 1000 hours and then raised significantly.

In cases of other two groups which were tempered at 875K and 975K, the shapes of transition curves are similar to that of the base metal (Fig.5(b) and (c)). The  $vTr_{30}$  of the specimen tempered at 875K is lowered at first and then raised with an increasing tempering time. The  $vTr_{30}$  of that tempered at 975K is raised simply with an increasing time.

#### (b) Change of transition temperature

Fig.6 shows the changes in transition temperatures  $vTr_{30}$  of nine groups of specimens tempered at 775K to 975K. It is believed that a quenched steel would simply increase its toughness and therefore, decrease transition temperature with a progressive tempering process. However, if this steel is embrittled in a certain temperature-time range, the transition temperature should be raised in this range. The transition temperature of the non-embrittled specimen at each tempering time is not known quantitatively; an imaginal value is shown tentatively by the dotted lines in Fig.6.

There are "hills" of  $vTr_{30}$  in each  $vTr_{30}$ -tempering time curve. Each independent hill will indicate the existence of an independent and different type of temper embrittlement. Three types of temper embrittlement are observed in the curve of the tempering temperature 775K (Fig.6 (a)), they are named tentatively the first, the second and the third types of embrittlement. The points  $S_2$  and  $S_3$  in the curve are considered to be the start points of the second and third types of embrittlement. Those three types of embrittlement are also seen in the curves of the tempering temperatures 800K and 825K (Fig.6 (b) and (c)). The time at which each of those embrittlement arises is shortened with a rising temperature.

The fourth type of embrittlement appears at 825K, it begins to arise at about 1000 hours of tempering (points  $S_4$ ; Fig.6 (c)). Three types of embrittlement are seen at 850K (Fig.6 (d)); those will meet the second, third and fourth types of embrittlement.

At 875K, however, no embrittlement is observed after the second type embrittlement disappears (the range DE in Fig.6 (e)). This state will correspond to "the de-embrittled state" which has been observed in the steel tempered above 875K[6]. The fourth type follows the de-embrittled state at 875K.

The de-embrittled state is observed in a wide time range at 900K (Fig.6 (f)) and all the time range at 925K (Fig.6 (g)).

At 965K and 975K, a new type of embrittlement (the fifth type) appears after the de-embrittled state (Fig.6 (h) and (i)).

### 4. Change of hardness during tempering

The hardness was measured on nine groups of specimens tempered at 775K to 975K

shown in Fig.7. The time points  $S_2$ ,  $S_3$ ,  $S_4$  and  $S_5$  in this figure are the start point of the second, third, fourth, fifth types of embrittlement shown in Fig.6. It is believed that a quenched steel

would be softened simply with the lapse of tempering time, if any special phenomenon of hardening would not occur. The dotted line attached to each figure is drawn imaging such a simple softening process. Fig.7 informs that there are certain relationships between the hardness and embrittlement of tempered specimens:

- (1) The hardness increases respectively when the first and second types of embrittlement occur (Fig.7 (a) and (b)). This fact suggests that the hardening of the specimen is the principal cause of inducing the first and second types of embrittlement.
- (2) The hardening in these cases will be caused by "the secondary hardening", which has been known as the phenomenon that a molybdenum-bearing steel, which has been softened by tempering with a shorter time, is hardened reversely by tempering with a longer time due to the precipitation of fine particles of molybdenum carbide [7,8].
- (3) The specimen may be hardened in some extent when the third type of embrittlement arises (Fig.7 (a) to (d)). In this case, however, the hardening mechanism is not yet clarified.
- (4) The specimen is not hardened when the fourth and fifth types of embrittlement arise as shown in Fig.7 (e),(f) and Fig.7 (h),(i), respectively.

#### 5. Change of fracture mode with progressive tempering process

Specimens fractured by Charpy impact test were used for SEM observation. Among the specimens used for a series of impact test, one which was fractured at the lowest temperature (95 to 143K) was used for the observation.

The fracture surfaces of seven typical specimens are shown in Fig.8. The fracture surface differs in appearance depending on the type of embrittlement arising in the specimens as follows.

- (1) First type (Fig.8 (a)): Specimen fractures with a cleavage mode. A continuous ridge is observed (arrow mark). This ridge may be the grain boundary of prior-austenite, and the fracture may initiate there. It is not yet clear whether the crack propagates along the cleavage planes or along the boundary of prior-martensite lathes.
- (2) Second type (Fig.8 (b)): The cleavage fracture and the ridge are observed. There is no essential difference between the fractures of Fig.8 (a) and (b), except that each cleavage plane surrounded by ridges is more flat in case of the latter.
- (3) Third type (Fig.8 (c)): The fracture of intergranular mode will be peculiar to the third type of embrittlement. Each fracture surface will meet the grain boundary of prior-austenite.

The area occupied by the intergranular fracture was measured on all over the fracture surface of a specimen. SEM observation was made with the magnifications of 100 and 200.

Fig.9 shows the percentage of intergranular fracture at each tempering time. The amount of intergranular fracture increases from the time point  $S_3$  (the start point of the third type of embrittlement) and reaches maximum just before the point  $S_4$  (the start point of the fourth type of embrittlement), and then decreases. This fact suggests that the third type will survive coexisting with the fourth type of embrittlement. The fracture obtained in this time range is shown in Fig.8 (d).

- (4) Fourth type (Fig.8 (e)): A cleavage fracture of flat surface is observed.
- (5) De-embrittled state (Fig.8 (f)): A cleavage fracture is observed.



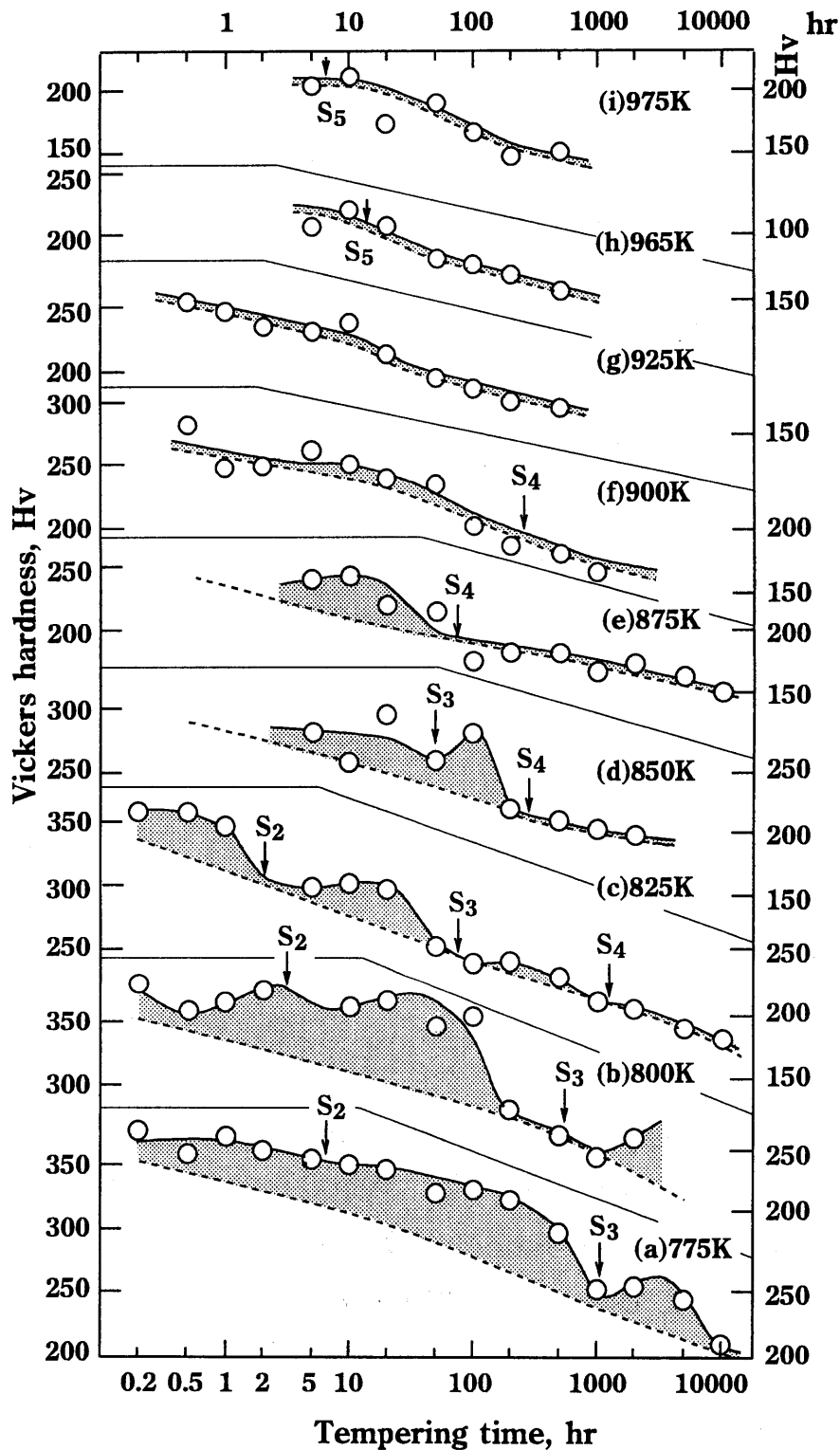
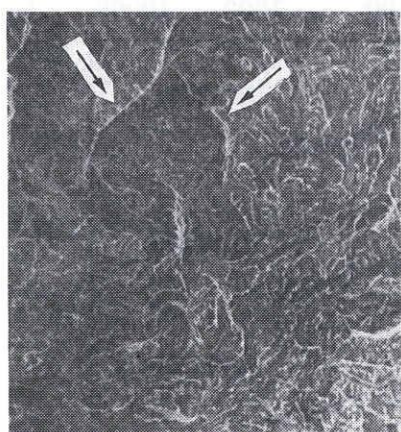
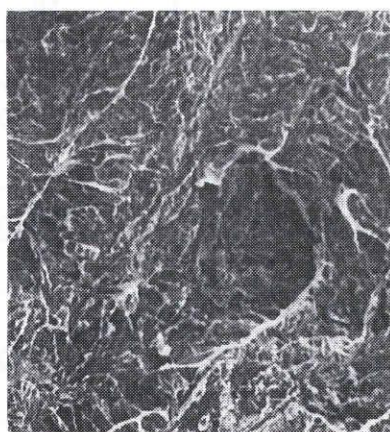


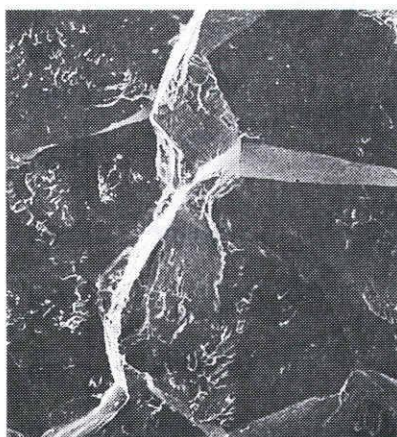
Fig.7 Change of hardness with the lapse of tempering time at 775K to 975K



(a) First type



(b) Second type



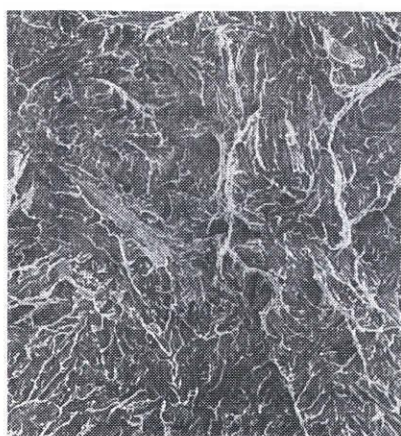
(c) Third type

(d) Mixture of third  
and fourth types

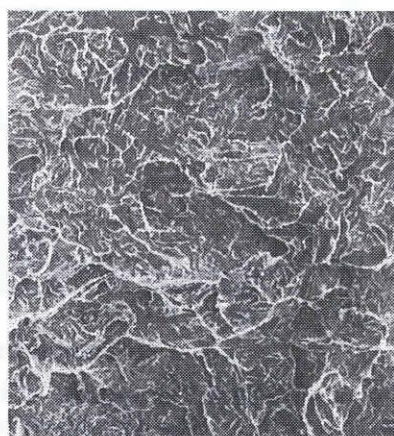
—|  
50  $\mu$ m

**Fig.8 Fracture surfaces of specimen**

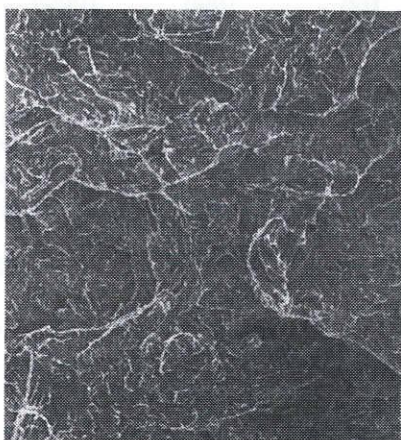
(a) 775K x 1hr, (b) 775K x 100hr, (c) 775K x 10000hr,  
(d) 825K x 10000hr, (e) 875K x 10000hr,  
(f) 925K x 500hr, (g) 975K x 500hr



(e) Fourth type



(f) De-embrittled  
state



(g) Fifth type

50  $\mu\text{m}$

**Fig.8 Continued**



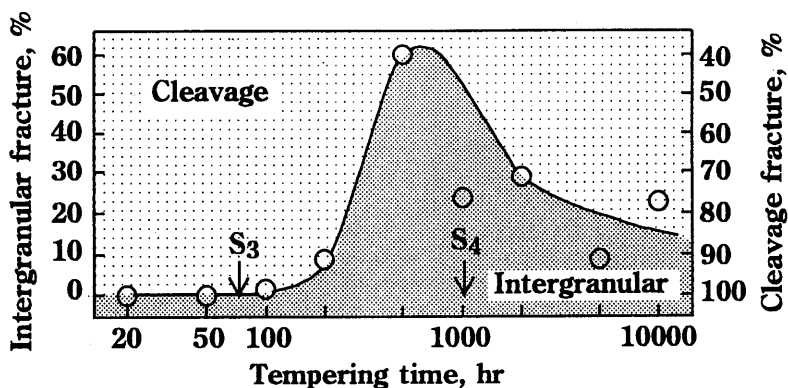


Fig.9 Percentage of intergranular fracture of the specimen in the embrittled states of third and fourth types of embrittlement; tempering temperature 825K

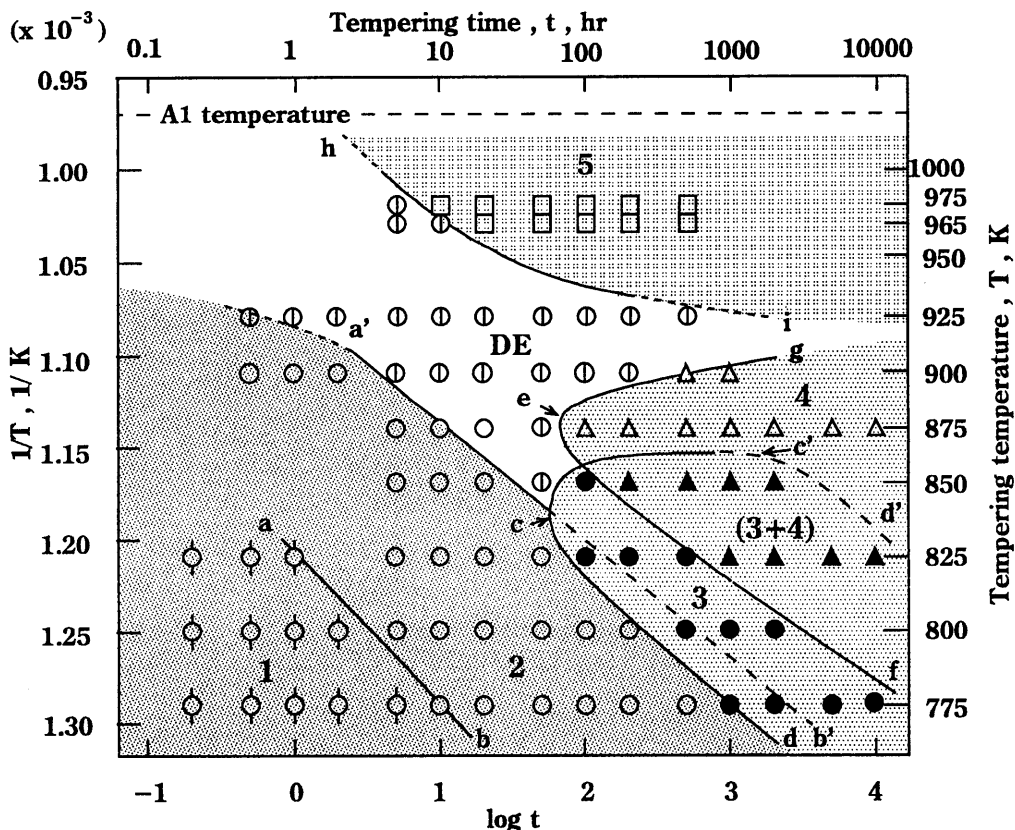


Fig.10 Time-temperature-embrittlement diagram;

Marks show the embrittled states of:

- first type, ○ second type, ● third type, △ fourth type,
- ▲ third and fourth types, □ fifth type and
- ⊙ de-embrittled state

(6)Fifth type (Fig.8 (g)): A cleavage fracture is observed.

#### 6. Time–temperature–embrittlement diagram

The time–temperature diagram, in which the arising ranges of the first to fifth types of embrittlement were specified, was constructed on the basis of the data in Fig.5, as shown in Fig.10. In this figure, the abscissa and the ordinate are divided at regular intervals of  $1/T$  and  $\log t$ , respectively;  $T(K)$  and  $t(hr)$  are also shown at the corresponding positions of the axes. The seven different plots in the figure indicate the embrittlement of:  $\emptyset$  the first type,  $\bigcirc$  the second type,  $\bullet$  the third type,  $\Delta$  the fourth type,  $\blacktriangle$  the mixture of third and fourth type,  $\square$  the fifth type. The plot  $\bigcirc$  shows that the specimen is not embrittled after the second type of embrittlement disappears. This region is shown by DE (de–embrittled state). Each boundary line shows:

ab and a'b': start and finish lines of the second type,

cd and cc': start and upper limit lines of the third type,(it may be disappear at c'd' line.)

ef and eg: start and upper limit lines of the fourth type,

hi: start line of the fifth type.

Those start and finish lines are given approximately by the following equations being based on the concept of the tempering parameter [9].

$$ab: T(\log t+18)=14.8 \times 10^3$$

$$cd: T(\log t+18)=16.3 \times 10^3$$

$$a'b': T(\log t+18)=16.6 \times 10^3$$

$$ef: T(\log t+18)=17.2 \times 10^3$$

$$c'd': T(\log t+18)=18.4 \times 10^3 \text{ (estimated)}$$

#### 7. Correspondence of the first to fifth types of embrittlement and the temper embrittlement in the previous researches

The authors pointed out the existence of five types of embrittlement and labeled them in the order of appearance in progressing tempering process (increasing time and rising temperature).

##### (1) The first and second types

The first or the second type arises as early tempering stage as 0.2 or 10 hours at 773K. Its characteristics seems to resemble to that of the "low temperature temper embrittlement" (LTTE, tempered martensite embrittlement or 350°C (623K) embrittlement) [2]. LTTE has been known to exhibit following characteristics: (a)It is observed in the range 470 to 670K. (b) Steels containing impurities such as phosphorus are susceptible to this type of embrittlement. (c) Cementite precipitation along grain boundary in conjunction with the redistribution of impurities might play a dominant role in the embrittlement. (d)The embrittlement is not reversible. (e)The mode of fracture is intergranular along the prior–austenite grain boundary.

The first and the second types do not always possess those characteristics, and hence, it will be concluded that these types of embrittlement would not correspond to LTTE.

With these types of embrittlement, little is known by the authors, except that; (a)although the mode of fracture of the first type is transgranular, the grain boundary of prior–austenite would play an important role for crack initiation, (b)loss of ductility in ferrite matrix which is caused by the secondary hardening would relate closely to the first and the

second types.

At present, little contributions are available with these types of embrittlement.

(2)The third type

The third type of embrittlement will be identical with "the reversible temper embrittlement (RTE, or simply "the temper embrittlement") [1,2] which has been observed in several alloy steels. RTE appears with the following characteristics [2]. (a)It arises when steels are heated in the temperature range around 870K or when cooled slowly through this range. (b)The fracture exhibits the intergranular mode along the grain boundary of prior-austenite. (c)The reaction is reversible, i.e., the embrittlement can be removed when the steel is heated above 870K. (d)Steels containing impurities such as phosphorus are highly susceptible to this type of embrittlement.

(3)The fourth type

The fourth type of embrittlement appears in the temperature range below about 900K after the long time tempering. This type coexists with the third type in some time-temperature range. The specimen in which this embrittlement arises produces the cleavage fracture of transgranular mode.

At present, little contributions are available with this embrittlement

(4)The fifth type

The fifth type of embrittlement is caused by tempering above 950K for more than 10 hours. This type may belong to "the upper-nose temper embrittlement" (UNTE) [2,10,11] of alloy steels. Following characteristics of UNTE have been reported. (a)It arises when tempering is carried out at the higher temperature approaching  $A_{c1}$ , typically above 900K, as in the case of stress relieving. (b)The fracture mode is transgranular cleavage (c)Embrittlement increases as the temperature is raised up to  $A_{c1}$  and therefore is essentially irreversible. (d)The magnitude of embrittlement is insensitive to the cooling rate from the tempering temperature. (e)Molybdenum enhances embrittlement, in the sense that brittleness appears at lower temperatures and for shorter times as the molybdenum content is increased. (f)The UNTE will occur due to the formation of very coarse molybdenum-rich  $M_{23}C_6$  carbides in the grain boundary which fracture upon plastic straining of the ferrite matrix and thus initiate premature cleavage cracking.

Kinoshita [3] examined "the SR embrittlement" of alloy steels which arises when the weldments are subjected to the stress relief annealing. Thermal cycles shown in Fig.11, which simulate some stress relieving processes of weldments, were given to the specimens. The fracture appearance transition temperature of the specimen obtained by each thermal cycle is shown below the ordinate. Experimental results inform following facts.

(a)A short-time exposure of the specimen at the stress relieving temperature (1000K x 1hr) does not raise the transition temperature of the de-embrittled specimen.

(b)A long-time exposure at the stress relieving temperature (975K x 100hr) raises the transition temperature remarkably.

(c)Slow cooling from the stress relieving temperature raises the transition temperature in some extent.

Kinoshita [3] concluded that the "SR embrittlement" is caused both in the process of the stress relieving itself and in the process of cooling.

The present authors consider that the embrittlement caused by the former process meets the fifth type of embrittlement(the UNTE) and that caused by the latter dose most possibly the third type(the RTE). It can be said, therefore, that "the fifth type of embrittle-

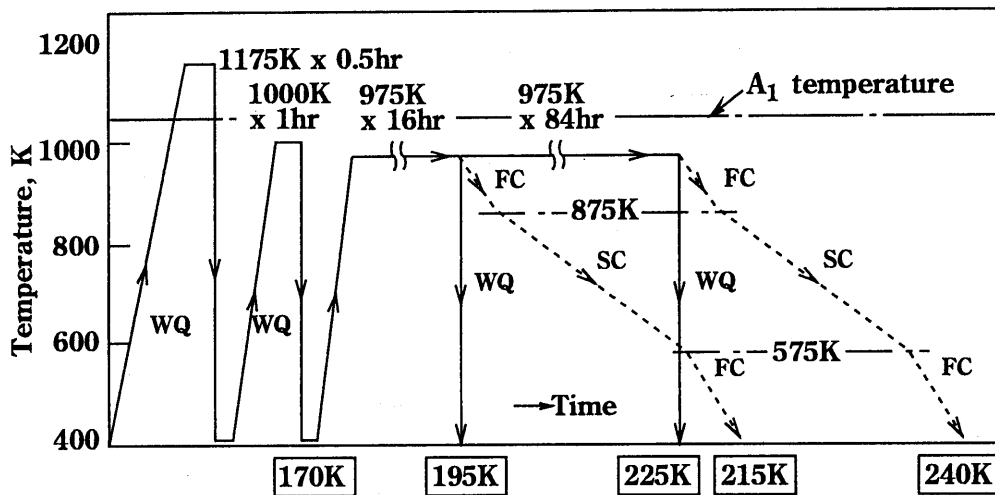


**Fig.11 Influence of several thermal cycles on the SR embrittlement and the temper embrittlement of 2 1/4Cr-1Mo steel (by Kinoshita [3])**  
**The fracture appearance transition temperature obtained by each thermal cycle is shown below the ordinate .**

**WQ:Water quenching, FC:Furnace cooling,  
 SC: Slow cooling with the cooling rate of 10K/hr**

ment (the UNTE)" corresponds to "the SR embrittlement in a narrow sense".

## 8. Conclusion

The temper embrittlement of HAZ of 2 1/4Cr-1Mo steel was examined. Experiments were made in the tempering temperature and time ranges 775 to 975K and 0.2 to 10000 hours. Each rise of the transition temperature was detected. The experimental results informed that there are five types of temper embrittlement. The time-temperature region where each of those embrittlement arises was shown graphically in a diagram. Five types of embrittlement show following characteristics.

- (1)The first and the second types appear in the earlier stage of tempering, such as 1 hour and 5 to 500 hours at 773K. The secondary hardening will relate closely to these types.
- (2)The third type arises after a longer-time tempering, such as 100 to 1000 hours at 825K. This embrittlement is identical with RTE.
- (3)The fourth type seems to arise in the final stage of tempering below 900K. Little works have been made to distinguish this embrittlement from RTE.
- (4)The fifth type is observed in the higher temperature range above 950K. This embrittlement will be identical with the UNTE and also the SR embrittlement in a narrow sense.

In case of the third type of embrittlement, an intergranular fracture is produced by the impact test at the lowest temperature, in other cases, a cleavage fracture was observed.

### Acknowledgments

This research was supported by The Grant-in-Aid for Scientific Research of The Ministry of Education, Japan.

The authors wish to thank Dr. Hirokazu Nomura, Former Director of Engineering Research Center of NKK Corporation for his support to this research.

The authors also thank Messrs. H. Inayoshi, K. Masuda, T. Ozaki, K. Kondo, and R. Ishida, the students of Mie University for their cooperations.

### References

- [1] T. Takamatsu et al: Temper embrittlement characteristics of 2 1/4Cr-1Mo steel, *Tetsu to Hagané*, 67-1(1981), 178-187 (in Japanese).
- [2] F.C. Pickering et al: *Materials Science and Technology*, VCH Verlags, (1992), Vol.7, pp.170-171, 461-463.
- [3] K. Kinoshita, H. Kaji, M. Katsumata: The relationship between stress relief embrittlement and temper embrittlement in low alloy steels, *Kobe Seiko Giho (R-D)*, 29-4(1979), 67-71 (in Japanese).
- [4] K. Tamaki, J. Suzuki et al: Temper embrittlement in HAZ of 1 1/4Cr-1/2Mo steel, *IIW Document IX-1665-92*, (1992, Madrid).
- [5] G.C.Gould: Long time isothermal embrittlement in 3.5Ni, 1.75Cr, 0.50Mo, 0.20C steel, *ASTM Special Technical Publication*, 407(1967), 90-105.
- [6] S.Sawada, T.Ohashi: The de-embrittlement behavior of a temper embrittled low alloy steel, *Tetsu to Hagané*, 62-6(1976), 644-651 (in Japanese).
- [7] K.Tamaki, J.Suzuki et al: Effect of carbides on reheat cracking sensitivity, *Trans. Japan Welding Soc.*, 15-1 (1984), 8-16.
- [8] K.Tamaki, J.Suzuki et al: Time-temperature-hardness diagrams of tempered steels, *Res. Rep. Fac. Eng. Mie Univ.*, Vol.15 (1990), 9-22.
- [9] F.R.Larson, J. Miller: A Time-temperature relationships for rupture and creep stresses, *Trans.ASME.*, 74-7 (1952), 765-775
- [10] L.D. Jaffe, D.C. Buffum: Upper nose temper embrittlement of a Ni-Cr steel, *Trans.AIME*, 209-1(1957), 8-16.
- [11] J.P. Naylor, M. Guttman: Mechanism of upper-nose temper embrittlement in Mn-Ni-Mo A533 gr.B steel, *Metal Science*, 15-10(1981), 433-441.